Appl Microbiol Biotechnol (2016) 100:2011–2021
DOI 10.1007/s00253-015-7052-9

ENVIRONMENTAL BIOTECHNOLOGY

Mechanisms and microbial structure of partial denitrification with high nitrite accumulation

Rui Du[1] · **Yongzhen Peng**[1] · **Shenbin Cao**[2] · **Baikun Li**[1] · **Shuying Wang**[1] · **Meng Niu**[1]

Received: 27 July 2015 / Revised: 23 September 2015 / Accepted: 29 September 2015 / Published online: 3 November 2015

Abstract Nitrite (NO_2^--N) accumulation in denitrification can provide the substrate for anammox, an efficient and cost-saving process for nitrogen removal from wastewater. This batch-mode study aimed at achieving high NO_2^--N accumulation over long-term operation with the acetate as sole organic carbon source and elucidating the mechanisms of NO_2^--N accumulation. The results showed that the specific nitrate (NO_3^--N) reduction rate (59.61 mg N VSS^{-1} h^{-1} at NO_3^--N of 20 mg/L) was much higher than specific NO_2^--N reduction rate (7.30 mg N VSS^{-1} h^{-1} at NO_3^--N of 20 mg/L), and the NO_2^--N accumulation proceeded well at the NO_3^--N to NO_2^--N transformation ratio (NTR) as high as 90 %. NO_2^--N accumulation was barely affected by the ratio of chemical oxygen demand (COD) to NO_3^--N concentration (C/N). With the addition of NO_3^--N, NO_2^--N accumulation occurred and the specific NO_2^--N reduction rate declined to a much lower level compared with the value in the absence of NO_3^--N. This indicated that the denitrifying bacteria in the system preferred to use NO_3^--N as electron acceptor rather than use NO_2^--N. In addition, the Illumina high-throughput sequencing analysis revealed that the genus of *Thauera* bacteria was dominant in the denitrifying community with high NO_2^--N accumulation and account for 67.25 % of total microorganism. This bacterium might be functional for high NO_2^--N accumulation in the presence of NO_3^--N.

Keywords Nitrite accumulation · Partial denitrification · Anammox · Nitrate-to-nitrite transformation ratio · Microbial community

Introduction

Conventional denitrification is a reduction process carried out by diverse bacteria under anoxic conditions and involves a series of reaction from NO_3^--N to dinitrogen gas (N_2), catalyzed by the nitrate reductase (*Nar*), nitrite reductase (*Nir*), nitric oxide reductase (*Nor*), and nitrous oxide reductase (*Nos*) (Eq. 1, Zumft 1997).

$$NO_3^-\text{-N} \xrightarrow{NaR} NO_2^-\text{-N} \xrightarrow{NiR} NO \xrightarrow{NoR} N_2O \xrightarrow{Nos} N_2 \quad (1)$$

As the major intermediate of NO_3^--N reduction process, NO_2^--N has been frequently reported to accumulate (Ge et al. 2012; Gong et al. 2013) which was harmful to natural water bodies (Zhou et al. 2011). In traditional biological nitrogen removal (BNR) processes, NO_2^--N leaving from the first denitrification will be oxidized in the subsequent aerobic nitrification and consume extra oxygen (Ge et al. 2012). It could also have inhibition on the nitrogen or phosphorus removal process (Ma et al. 2013). However, anaerobic ammonium oxidation (anammox) has been developed as an efficient and cost-saving BNR process recently, in which NO_2^--N is needed as one of the substrates (Mulder et al. 1995). Therefore, the anammox process could be combined with heterotrophic denitrification with NO_2^--N accumulation (Waki et al. 2013; Kalyuzhnyi et al. 2006).

Electronic supplementary material The online version of this article (doi:10.1007/s00253-015-7052-9) contains supplementary material, which is available to authorized users.

✉ Yongzhen Peng
pyz@bjut.edu.cn

[1] Engineering Research Center of Beijing, Key Laboratory of Beijing for Water Quality Science and Water Environment Recovery Engineering, Beijing University of Technology, Pingleyuan 100, Chaoyang District, Beijing 100124, People's Republic of China

[2] State Key Laboratory of Urban Water Resource and Environment, Harbin Institute of Technology, Harbin 150090, China

A number of environmental factors could affect NO_2^--N accumulation, including C/N (Oh and Silverstein 1999; Ge et al. 2012), carbon source type (Ge et al. 2012; Rijn et al. 1996), and pH (Glass and Silverstein 1998). Denitrification was inhibited when the pH was 6.5 or 7.0, and the peak value of NO_2^--N accumulation increased at pH of 9.0 as reported by Glass and Silverstein (1998). However, the NO_2^--N accumulation was more serious at low pH than at high pH condition in the study of Cao et al. (2013a). NO_2^--N accumulation in denitrification was also impacted by the types of carbon sources rather than C/N ratio (Sun et al. 2009), and accumulation of NO_2^--N was found at acetate-limited denitrification (Oh and Silverstein 1999). The tests of partial denitrification under acetate feast-famine condition showed that readily biodegradable chemical oxygen demand (COD) to NO_3^--N (RBCOD/NO_3^--N) ratio of 2.5 facilitated an ideal NO_2^--N accumulation ratio of 71.7 % (Gong et al. 2013).

Until now, the understanding of NO_2^--N accumulation during denitrification is still unclear. A kinetic model based on competitive inhibition of NO_2^--N reduction by NO_3^--N predicted that NO_2^--N accumulation was the result of competition between NO_3^--N and NO_2^--N reductase for the electrons generated by the oxidation of electron donors (Almeida et al. 1995). NO_2^--N accumulation was also reported to be associated with the limited substrate electron flow to NO_2^--N reductase (Almeida et al. 1995; Rijn et al. 1996). Other study found that NO_2^--N accumulation was caused by the delayed synthesis of NO_2^--N reductase relative to NO_3^--N reductase (Blaszczyk 1993). Moreover, NO_2^--N accumulation is strongly affected by the microbial species composition. Three groups of NO_3^--N reducing bacteria was involved with respect to their capability of reducing NO_3^--N and NO_2^--N (Martienssen and Schöps 1997), the first group of reducing NO_3^--N only to NO_2^--N, the second group of reducing NO_3^--N and NO_2^--N without any NO_2^--N accumulation, and the third group of reducing NO_3^--N associated with a transient accumulation of NO_2^--N. Different microorganisms possessed various patterns of NO_2^--N accumulation, and NO_2^--N accumulation was strongly influenced by microbial species (Blaszczyk 1993).

A high NO_2^--N accumulation denitrifying sludge was obtained with the NTR up to 80 % (Cao et al. 2013b), which was much higher than previous reported values (Ge et al. 2012; Gong et al. 2013; Sun et al. 2009). However, the mechanisms for NO_2^--N accumulation were still unclear. Therefore, the objective of this study was to elucidate the mechanisms of high NO_2^--N accumulation in denitrification through sequencing batch rector (SBR) tests and lab-scale batch tests. The denitrification activity (e.g., NO_3^--N and NO_2^--N reduction rate) was determined with acetate as carbon source. Microbial community was characterized for high NO_2^--N accumulation by Illumina high-throughput sequencing analysis. Finally, the potential of combining the partial denitrification with anammox for advanced BNR processes was discussed.

Materials and methods

SBR and operation

Denitrification tests were conducted in a laboratory-scale SBR (working volume 5 L) operated at room temperature (16.0~28.0 °C) with two cycles per day, with each cycle consisting of 10-min feeding with NO_3^--N-contained wastewater, 1-min feeding carbon source, 30-min settling, and 9-min discharging. The initial C/N was set as 3.0. The anoxic reaction time for denitrification was shortened from 40 to 20 min in order to obtain sufficient NO_2^--N accumulation. The reactor was mixed using a mechanical stirrer at 100 rpm. The SBR reactor was operated without sludge discharge during the 74-day operation period.

The seeding sludge in the SBR reactor was taken from a denitrifying reactor with sludge fermentation liquid as organic carbon source, which possessed the high NO_2^--N accumulation property and maintained stable performance with NO_2^--N transformation ratio of 80 % during 108-day operation period (Cao et al. 2013a). The SBR reactor was fed with synthetic wastewater containing NO_3^--N and mineral solutions, and the composition was 182.1 mg/L $NaNO_3$ (30 mg/L NO_3^--N), 11.1 mg/L KH_2PO_4, 6 mg/L $MgSO_4{\cdot}7H_2O$, 3 mg/L $CaCl_2{\cdot}2H_2O$, and 1 mL trace element solution. The trace element solution contained 1.5 g/L $FeCl_3{\cdot}6H_2O$, 0.03 g/L $CuSO_4{\cdot}5H_2O$, 0.12 g/L $MnCl_2{\cdot}4H_2O$, 0.06 g/L $Na_2MoO_4{\cdot}2H_2O$, 0.12 g/L $ZnSO_4{\cdot}7H_2O$, 0.15 g/L $CoCl_2{\cdot}6H_2O$, 0.18 g/L KI, 0.15 g/L H_3BO_3, and 10 g/L EDTA. Sodium acetate solution (5 g COD/L) was used as the organic carbon source to supply the electron donor for NO_3^--N reduction.

Batch experiments

Besides the SBR reactor, several sealed conical flask reactors (0.5 L) were used for batch tests. Liquid-phase samples were taken from each flask using a sterile injector (20 mL). All of the batch tests were carried out in a temperature incubator at 25±0.5 °C, and the reactors were stirred at 250 rpm. At the start of each test, the reactor was filled up with fresh mixed liquor taken from the SBR during the anoxic reaction phase. Then, the mixture was washed three times by discarding the supernatant and adding deionized water and finally diluted with deionized water to 0.5 L. The reactors were purged with nitrogen gas for 10 min and covered with the sealing film to ensure anoxic condition for denitrification. Three batch experiments were carried out to investigate the characteristic of denitrification with high NO_2^--N accumulation.

First experiment, batch tests were conducted to investigate the denitrification properties (NO_3^--N reduction rate, NO_2^--N accumulation rate, and NO_2^--N reduction rate) under unlimited carbon source condition. At the beginning of each test, NO_3^--N stock solution (10 g N/L) was added into the reactor

to achieve initial NO_3^--N concentrations of 20, 40, 80, and 150 mg N/L, respectively. Sodium acetate solution was added into the reactors with the initial C/N of 5.0. During the batch tests of 60~120 min, 10 mL mixed liquor samples were taken every 5~20 min for the analysis of NO_3^--N, NO_2^--N, and COD.

Second experiment, the effect of C/N ratios on denitrification was investigated under limited carbon source condition. At the beginning of each test, the NO_3^--N stock solution (10 g N/L) was added into the reactor to achieve the initial NO_3^--N concentration of 20 mg N/L. Sodium acetate stock solution was then added for the initial COD concentrations of 16, 32, 48, 64, 80, and 160 mg COD/L, resulting in C/N ratios of 0.8, 1.6, 2.4, 3.2, 4.0, and 8.0, respectively. Each test lasted for 60 min.

Third experiment, the effect of NO_3^--N addition on NO_2^--N reduction was investigated. The NO_3^--N stock solution and NO_2^--N stock solution were added to the reactor at the beginning of each test to achieve the NO_x^--N (NO_3^--N + NO_2^--N) concentration of 40 mg N/L. The ratios of NO_3^--N/NO_2^--N were 3:1, 1:1, and 1:3, respectively. Sodium acetate stock solution was then added to the reactors to achieve the initial COD/NO_x^--N ratio of 3.0. Then, NO_3^--N was added in the middle phase of reaction when the NO_2^--N was reduced to a certain concentration. Two NO_2^--N concentrate solutions were prepared at 20 and 40 mg N/L, respectively. Sodium acetate was then supplied to the reactors to achieve the initial COD/NO_2^--N ratios of 3.0. After NO_2^--N was reduced for 10 or 20 min, NO_3^--N was added to 20 mg N/L in each reactor. The mixed liquor volatile suspended solids (MLVSS) concentration was measured at the beginning and the end of each test. All the batch tests were conducted in triplicate.

Calculation methods for denitrification activity and NO_2^--N accumulation

The two-step denitrification model was used in this study due to high NO_2^--N accumulation (Ni and Yu 2008) (Eq. 2). NO_3^--N is firstly converted to NO_2^--N and then reduced to N_2. NO_2^--N accumulation was the result of the lower NO_2^--N reduction rate than NO_3^--N reduction rate.

$$NO_3^- - N \rightarrow NO_2^- - N \rightarrow N_2 \tag{2}$$

The specific NO_3^--N reduction rate ($\mu_{NO3\text{-}N}$), specific NO_2^--N accumulation rate ($\mu_{NO2\text{-}N,\ Accu}$), specific NO_2^--N reduction rate at the present of NO_3^--N ($\mu_{NO2\text{-}N}$), and specific NO_2^--N reduction rate at the absent of NO_3^--N ($\acute{u}_{NO2\text{-}N}$) were determined through linear regression of NO_3^--N and NO_2^--N profiles and then divided by the MLVSS (Eqs. 3, 4, 5, and 6).

$$\mu_{NO3-N} = -dC_{NO3}/dt/VSS \tag{3}$$

$$\mu_{NO2-N,Accu} = dC_{NO2}/dt/VSS \tag{4}$$

$$\mu_{NO2-N} = \mu_{NO3-N} - \mu_{NO2-N,Accu} \tag{5}$$

$$\mu'_{NO2-N} = -dC_{NO2}/dt/VSS \tag{6}$$

where C_{NO3} and C_{NO2} were represented for the NO_3^--N and NO_2^--N concentration, respectively.

The NO_3^--N to NO_2^--N transformation ratio (NTR) was calculated with three methods at different situation as follows:

1. A typical cycle of long-term operation (NTR_T)

$$NTR_T(\%) = \left(NO_2^-\text{-}N_t - NO_2^-\text{-}N_{initial}\right) / \left(NO_3^-\text{-}N_{initial} - NO_3^-\text{-}N_t\right) \times 100\% \tag{7}$$

where NO_2^--N_t and NO_2^--$N_{initial}$ were the NO_2^--N concentrations at the sampling point and the initial concentration, respectively. NO_3^--N_t and NO_3^--$N_{initial}$ were the NO_3^--N concentrations at the sampling point and the initial concentration, respectively.

2. Long-term operation of the SBR reactor (NTR_L)

$$NTR_L(\%) = \left(NO_2^-\text{-}N_{eff} - NO_2^-\text{-}N_{initial}\right) / \left(NO_3^-\text{-}N_{initial} - NO_3^-\text{-}N_{eff}\right) \times 100\% \tag{8}$$

where NO_2^--N_{eff} and NO_2^--$N_{initial}$ were the NO_2^--N concentrations of the effluent and the initial phase, respectively. NO_3^--N_{eff} and NO_3^--$N_{initial}$ were the NO_3^--N concentrations of the effluent and the initial phase, respectively.

3. Batch experiments (NTR_B)

$$NTR_B(\%) = \mu_{NO2-N,Accu}/\mu_{NO3-N} \times 100\% \tag{9}$$

where $\mu_{NO2\text{-}N,\ Accu}$ and $\mu_{NO3\text{-}N}$ were the specific NO_2^--N accumulation rate and specific NO_3^--N reduction rate, respectively.

Analytical methods

The influent and effluent samples were collected on daily basis and were analyzed immediately. NO_2^--N and NO_3^--N were measured with a Lachat QuikChem 8500 Flow Injection Analyzer (Lachat Instruments, Milwaukee, USA), and COD was analyzed using a COD quick-analysis apparatus (Lianhua Tech. Co., Ltd., 5B-1, China). The MLSS and MLVSS of activated sludge were measured according to the Standard Methods (APHA 1998).

DNA extraction and PCR

DNA sample was extracted from 0.10~0.20 g dried sludge using the Fast DNA Kit (BIO 101, Vista, CA) according to the manufacturer's instruction (Du et al. 2014). DNA concentrations were measured with a NanoDrop ND-1000 (NanoDrop Technologies, DE, USA).

Polymerase chain reaction (PCR) was conducted to amplify the 16S ribosomal RNA (rRNA) gene. Primers for sequencing were 515F (5′-GTGCCAGCMGCCGCGG-3′) and 907R (5′-CCGTCAATTCMTTTRAGTTT-3′) for the V4 and V5 region of 16S rRNA gene. The PCR was performed in a mixture (20 μL) containing 4 μL 5× FastPfu buffer, 2 μL dNTPs (2.5 mM), 0.8 μL of forward primer (5 μM), 0.8 μL of reverse primer (5 μM), 0.4 μL FastPfu polymerase (TransGen Biotech, China), 10 ng of template DNA, and deionized water. The thermal programs of PCR consisted of an initial denaturation at 95 °C for 3 min, followed by 27 cycles of denaturing at 95 °C for 30 s, annealing at 55 °C for 30 s, and extension at 72 °C for 45 s, followed by a final extension at 72 °C for 10 min. The products were analyzed by gel electrophoresis using 2 % (*w*/*v*) agarose.

High-throughput sequencing data analysis

The PCR products were quantified by GeneAmp® 9700 PCR system (ABI, USA) and finally analyzed for sequencing by Illumina MeSeq PE250 platform (Illimina, USA). In order to minimize the impact of potential early round PCR errors, amplicon libraries were prepared by combining three independent PCR products. Equal amount of purified amplication products were sent to Shanghai Majorbio Biopharm Biotechnology Co., Ltd. (Shanghai, China) for pyrosequencing. The trimmed sequences were grouped into operational taxonomic units (OTUs) using 97 % identity thresholds (i.e., 3 % dissimilarity levels) by the Usearch software program. The OTU numbers were counted for the sample as the species richness, and rarefaction curves and Shannon-Wiener were generated. The generated raw sequences of the sludge sample were assigned by Silva (http://www.arb-silva.de) to trim off the adapters and barcodes. All the raw reads have been archived at NCBI Sequence Read Archive (SRA) database with accession number of SRR2106467.

Results

Acclimatization with acetate as carbon source

The seeded denitrifying sludge originally used the sludge fermentation liquid as carbon source, which contained plenty of short-chain fatty acids (SCFAs), polysaccharide, and protein, with the soluble chemical oxygen demand (SCOD) of 3021 mg/L. The C/N was set at 3.0 in denitrification and the NTR_L achieved 80 % during108-day operational period (Cao et al. 2013b).

In order to enrich the NO_2^--N accumulation denitrifying sludge, the carbon source was replaced by sodium acetate with C/N of 3.0. The variation of NO_3^--N, NO_2^--N, NTR_L, and temperature was studied during the 74-day operational period (Fig. 1a). Results showed that the high NO_2^--N accumulation was maintained stably and NTR_L was around 80 % with acetate as the sole carbon source and temperature ranging from 16 to 28.5 °C.

A typical cycle for NO_3^--N reduction and NO_2^--N accumulation was demonstrated (Fig. 1b). During the denitrification process, NO_3^--N decreased gradually with the consumption of organic matters. NO_2^--N accumulated and reached the peak value at approximately 35 min after the reaction, and the NTR_T was up to 90 %. In order to investigate the NO_2^--N reduction in the absence of NO_3^--N, the reaction time was prolonged to 60 min for this cycle. After NO_3^--N was consumed completely, the accumulated NO_2^--N declined slowly in the last 20 min mainly due to the heterotrophic reduction using the internal carbon source as the electron donor.

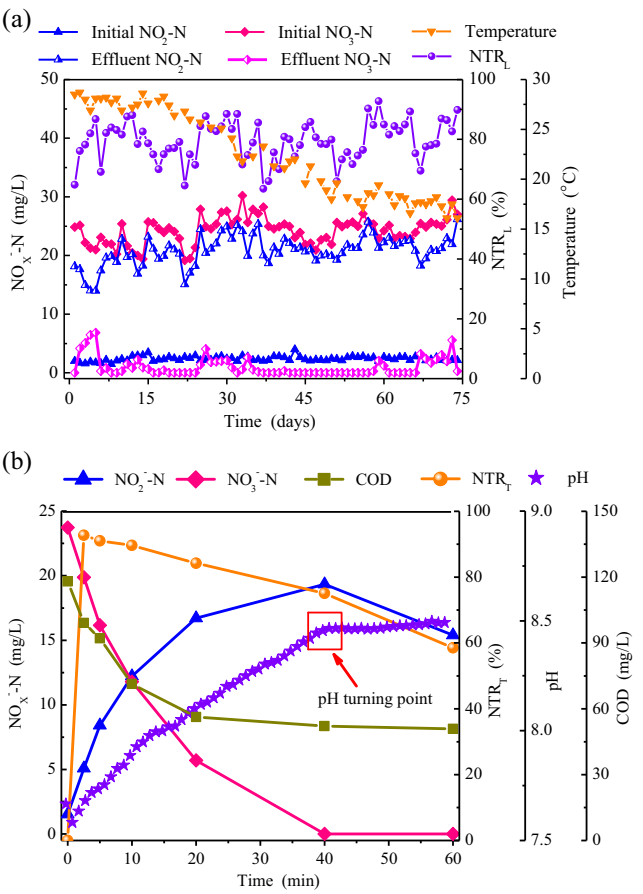

Fig. 1 **a** Variations of nitrogen concentration and temperature in the SBR reactor over the long-term operation period (74 days) and **b** variation of NO_3^--N, NO_2^--N, COD, NTR_T, and pH in a typical cycle

Correspondingly, the NTR_T decreased from 90 to 60 %, which indicated that terminating the denitrification reaction on time was critical for preventing the accumulated NO_2^--N from being reduced and achieving the highest NO_2^--N production.

The pH could be chosen as a controlled parameter for the reaction ending point as depicted (Fig. 1b). Theoretically, alkalinity production did not occur in the reduction of NO_3^--N to NO_2^--N but in the second step from NO_2^--N reduction to N_2 (Ge et al. 2012). Therefore, the pH would not ascend during the NO_2^--N accumulation period. However, the result in this study clearly showed the increase in pH, which was caused by the OH^- production from the consumption of sodium acetate (Eq. 10), so that the increase of pH during the NO_2^--N accumulation period was mainly attributed to the consumption of organic carbon, rather than the alkalinity production from denitrification. Similar result had been found that the pH could be used as a suitable indicator to estimate substrate feast-famine condition (Gong et al. 2013).

$$CH_3OO^- + H_2O \rightarrow CH_3OOH + OH^- \quad (10)$$

NO_2^--N accumulation of 90 % was much higher than the previous study (Ge et al. 2012), which found that NO_2^--N accumulation accounted for 21 % of total nitrogen by adding acetic acid in each anoxic denitrification zone of a modified UCT step feed BNR process. The mechanisms of high and stable NO_2^--N accumulation in this study were further explored in the following batch experiments.

Denitrification activities with unlimited carbon sources

NO_3^--N reduction and NO_2^--N accumulation with different initial concentrations were examined under the unlimited carbon source condition. The rapid increase in NO_2^--N was observed right after the reaction started (Fig. 2) and then reached a peak value varied from 13.4 to 130.88 mg/L with different NO_3^--N. Subsequently, the accumulated NO_2^--N decreased gradually due to the reduction with excess carbon source as the electron donor. Notably, the NO_2^--N accumulated peak was closely related to the NO_3^--N exhaustion point, before which there was approximately 90 % NO_3^--N being converted to NO_2^--N. NO_3^--N decrease and NO_2^--N accumulation appeared to be a linear relationship with time. Therefore, the specific denitrification activities could be determined by the variation of NO_2^--N or NO_3^--N concentrations and MLVSS

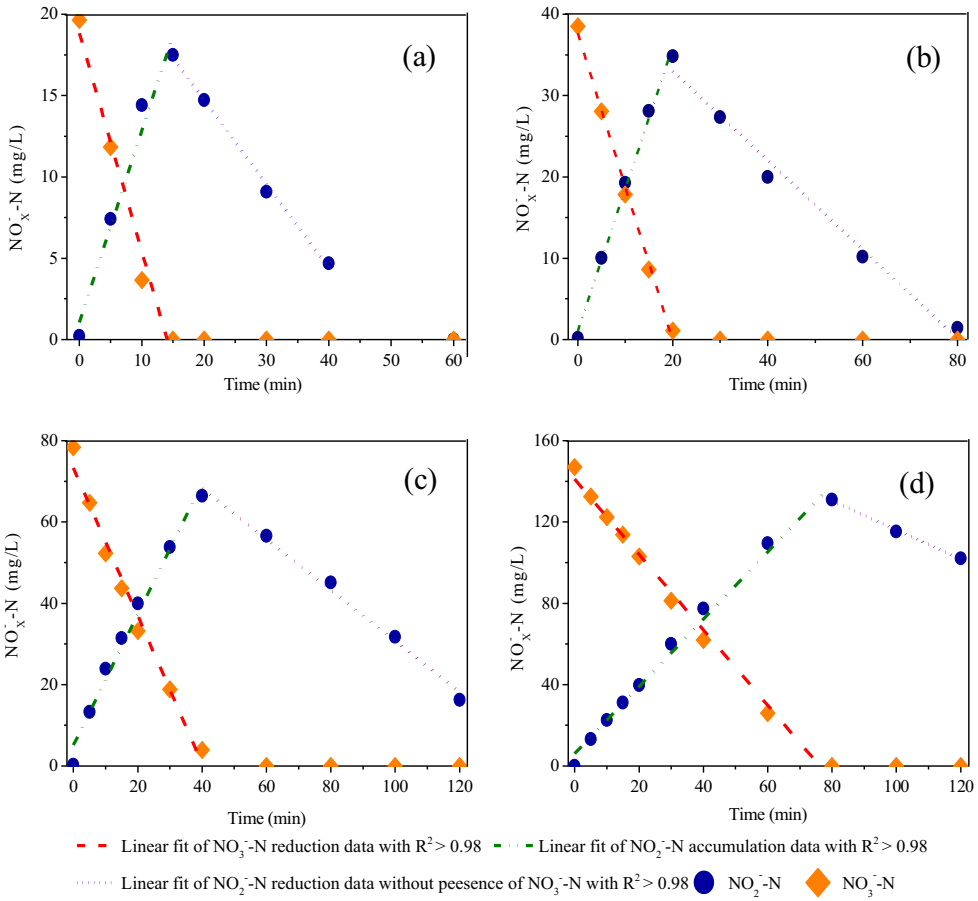

Fig. 2 Variations of NO_3^--N and NO_2^--N under unlimited carbon source at different NO_3^--N concentration: **a** NO_3^--N of 20 mg/L, **b** NO_3^--N of 40 mg/L, **c** NO_3^--N of 80 mg/L, and **d** NO_3^--N of 150 mg/L

Table 1 Properties and kinetic analysis of high NO_2^--N accumulation with different NO_3^--N concentrations

NO_3^--N (mg N L^{-1})	$\mu_{NO3\text{-}N}$ (mg N VSS^{-1} h^{-1})	$\mu_{NO2\text{-}N,\ Accu}$ (mg N VSS^{-1} h^{-1})	$\mu_{NO2\text{-}N}$ (mg N VSS^{-1} h^{-1})	$\acute{u}_{NO2\text{-}N}$ (mg N VSS^{-1} h^{-1})	$\mu_{NO3\text{-}N}$ /$\mu_{NO2\text{-}N}$	$\acute{u}_{NO2\text{-}N}$ /$\mu_{NO2\text{-}N}$	NTR_B (%)[a]
20	59.61	52.31	7.30	22.96	8.17	3.15	87.76
40	77.96	69.29	8.67	22.70	9.00	2.62	88.89
80	80.86	71.51	9.35	27.81	8.65	2.97	88.44
150	82.31	73.51	8.80	31.96	9.36	3.63	89.31

[a] NTR_B was calculated before nitrate was reduced completely

concentration in order to elucidate different denitrification steps.

Specific NO_3^--N reduction rate ($\mu_{NO3\text{-}N}$) increased with NO_3^--N concentration (Table 1). NO_3^--N reduction rate was much higher than the NO_2^--N reduction rate when NO_3^--N was present at all tests. With the initial NO_3^--N concentration of 40 mg N/L, the $\mu_{NO3\text{-}N}$ was 77.96 mg N VSS^{-1} h^{-1}, which was ninefold higher than the $\mu_{NO2\text{-}N}$ (8.67 mg N VSS^{-1} h^{-1}), and led to a high efficiency of NO_2^--N accumulation with the $\mu_{NO2\text{-}N,\ Acc}$ up to 69.29 mg N VSS^{-1} h^{-1}. This indicated that the NO_2^--N accumulation could be the result of the difference between NO_2^--N reduction rate and NO_3^--N reduction rate. Furthermore, NO_2^--N reduction rate (22.70 mg N VSS^{-1} h^{-1}) became higher when NO_3^--N was absent than that with NO_3^--N present (8.67 mg N VSS^{-1} h^{-1}). At the initial NO_3^--N concentration of 80 mg N/L, the $\acute{u}_{NO2\text{-}N}$ (27.81 mg N VSS^{-1} h^{-1}) was almost three times higher than the $\mu_{NO2\text{-}N}$ (9.35 mg N VSS^{-1} h^{-1}) in the presence of NO_3^--N, which confirmed that NO_3^--N was more favorable as the electron acceptor than NO_2^--N during the denitrification process.

Nitrate reduction and nitrite accumulation at various C/N ratios

After the tests of NO_2^--N accumulation with high $\mu_{NO2\text{-}N,\ Accu}$ at unlimited carbon sources, different C/N ratios were examined since it has been found as an important factor for NO_3^--N and NO_2^--N reduction (Ge et al. 2012). Therefore, the denitrification process with high NO_2^--N accumulation at different C/N ratios was investigated. High NO_2^--N accumulation occurred under limited carbon sources (e.g., C/N=0.8, 1.6, and 2.4) and under sufficient carbon sources (e.g., C/N=3.2, 4, and 8) (Fig. 3). The highest $\mu_{NO3\text{-}N}$ and $\mu_{NO2\text{-}N,\ Accu}$ were obtained by the linear regression of nitrogen compounds over the reaction time with R^2>0.95. The results showed that the $\mu_{NO3\text{-}N}$ was positively correlated with the C/N ratios (0.8–8.0), and the $\mu_{NO3\text{-}N}$ was much higher than the $\mu_{NO2\text{-}N}$ at all the C/N ratios tested (Fig. 4).

The maximum NTR_B at each C/N condition was up to 90 %, which clearly indicated that the C/N ratio did not affect the NO_2^--N accumulation in the denitrification process and

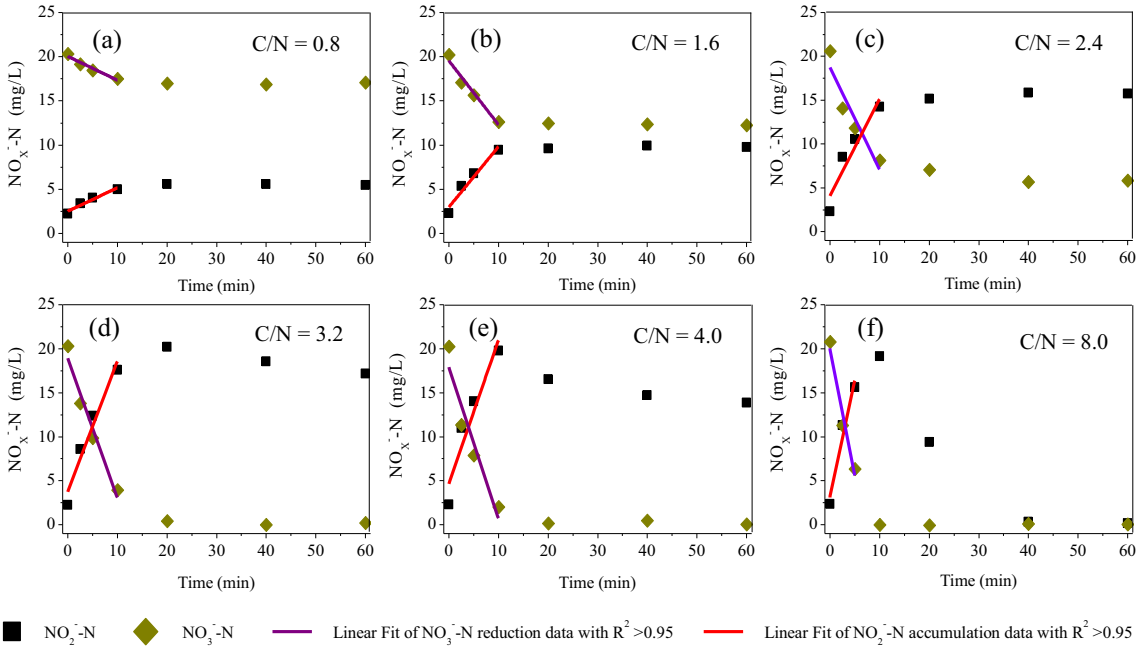

Fig. 3 Variations of NO_3^--N and NO_2^--N during denitrification tests with different C/N ratios (**a** C/N of 0.8, **b** C/N of 1.6, **c** C/N of 2.4, **d** C/N of 3.2, **e** C/N of 4.0, and **f** C/N of 8.0)

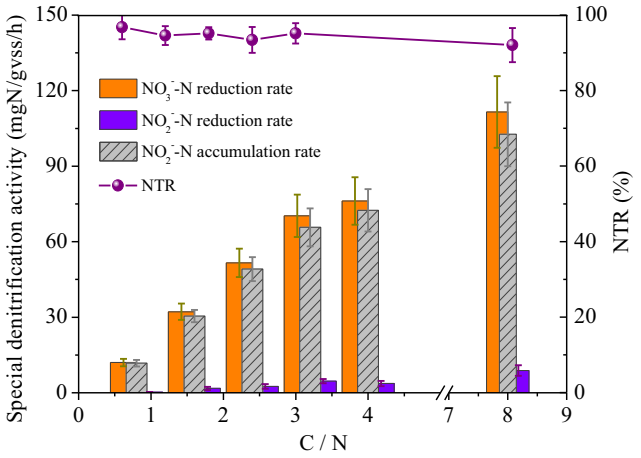

Fig. 4 Variation of specific NO_3^--N reduction rate, specific NO_2^--N accumulation rate, specific NO_2^--N reduction rate, and NTR_B before the complete reduction of NO_3^--N

NO_3^--N was still more favorable to be reduced than NO_2^--N even though sufficient electron donor was present. These results were different from previous studies, which found that high amount of NO_2^--N was accumulated either at low C/N (Her and Huang 1995) or high C/N (Ge et al. 2012). The discrepancy suggested that limited carbon source during denitrification was not the key factor for high NO_2^--N accumulation, and efficient NO_2^--N accumulation could be achieved within a wide range of organic carbon concentrations.

Effect of nitrate addition on nitrite reduction

Because NO_3^--N was more favorable as the electron acceptor than NO_2^--N, the effect of simultaneous supply of NO_3^--N and NO_2^--N on denitrification was further investigated to compare the reduction of NO_3^--N and NO_2^--N. NO_3^--N and NO_2^--N were added with the NO_3^--N to NO_2^--N ratios of 3:1, 1:1, and 1:3, respectively. NO_2^--N concentration increased gradually before the depletion of NO_3^--N (Fig. 5a–c), followed by the reduction of the accumulated NO_2^--N after the depletion of NO_3^--N. The $\mu_{NO3\text{-}N}$ was much higher than the $\mu_{NO2\text{-}N}$ at the initial period (Table 2) and declined with the decrease in NO_3^--N addition. The $\mu_{NO3\text{-}N}$ and $\mu_{NO2\text{-}N,\ Accu}$ declined, but the NTR_B stabilized at 92.29~95.68 % (Table 2).

Because NO_3^--N reduction was favored as electron acceptor than NO_2^--N when both of them were supplied (Fig. 5a–c), NO_3^--N was added when the NO_2^--N was reduced to some extent. NO_2^--N decreased with high $\acute{u}_{NO2\text{-}N}$ in the initial period compared (Fig. 5d, e). However, the reduction rate dropped sharply once NO_3^--N was added (Fig. 5f). With the initial NO_2^--N concentration of 20 mg N/L, the $\acute{u}_{NO2\text{-}N}$ was as high as 32.4 mg N L^{-1} h^{-1} at the beginning of the tests but rapidly decreased to 4.73 mg N L^{-1} h^{-1} after NO_3^--N addition at the10 min (Fig. 5d). This demonstrated that NO_2^--N reduction would be impeded in the presence of NO_3^--N and lead to NO_2^--N accumulation until the depletion of NO_3^--N.

Microbial diversity of high nitrite accumulation denitrifying sludge

High-throughput sequencing technique provides enough sequencing depth to cover the complex microbial communities (Shendure and Ji 2008). Pyrosequencing using the16S rRNA gene as the biomarker was conducted to examine the bacterial diversity of the sludge. Pyrosequencing of sludge sample yielded 17,786 effective sequences with average length of 396.27 bp. The Shannon value of 1.60 was obtained. There were 18 different groups at the phylum taxonomic rank (Fig. S1). *Proteobacteria* was the most abundant phylum in the sample, accounting for 75.87 % of total effective bacterial sequences. Other dominant phylum were *Bacteroidetes* (9.41 %), *Nitrospirae* (6.03 %), *Chlorobi* (2.13 %), and *Chloroflexi* (0.56 %) (Fig. S1).

At the genus level, the most abundant genus was *Thauera* (67.25 %) which was a member of the *β-Proteobacteria* and family *Rhodocyclaceae* (Fig. 6). Moreover, uncultured *Saprospiraceae* genus belonging to *Bacteroidetes* phylum accounted for 8.16 %. Bacteria belonging to *Candidate division OP3* of 2.84 % were detected. *Comamonadaceae* bacterium in belonging to *β-Proteobacteria* was also identified with 0.25 % in the system. Other denitrifying bacteria identified in the sludge were *Dechloromonas* (1.14 %) in β-Proteobacteria and *Denitratisome* (0.61 %). Additionally, there was 6 % of *Nitrospira* genus capable of converting NO_2^--N to NO_3^--N.

Discussion

Mechanisms of high nitrite accumulation in denitrification

The major reason for NO_2^--N accumulation was that the NO_2^--N reduction rate was much lower than NO_3^--N reduction rate. However, since denitrification is a microbial process involving several steps catalyzed by individual reductase enzymes, the interpretation for NO_2^--N accumulation was correlated with the considerably lower activity of NO_2^--N reduction enzymes than NO_3^--N reduction enzymes. Denitrifying enzymes require electrons produced by the oxidation of organic matters, and there was a competition for the electron supply among these enzymes (Pan et al. 2013). The C/N ratio showed little influence on NO_2^--N accumulation with the NTR_B maintaining at the high level about 90 % (Fig. 4), which indicated that the competition between NO_3^--N reductase and NO_2^--N reductase was not affected by C/N ratio. In other words, the C/N ratio was not an immediate cause for the

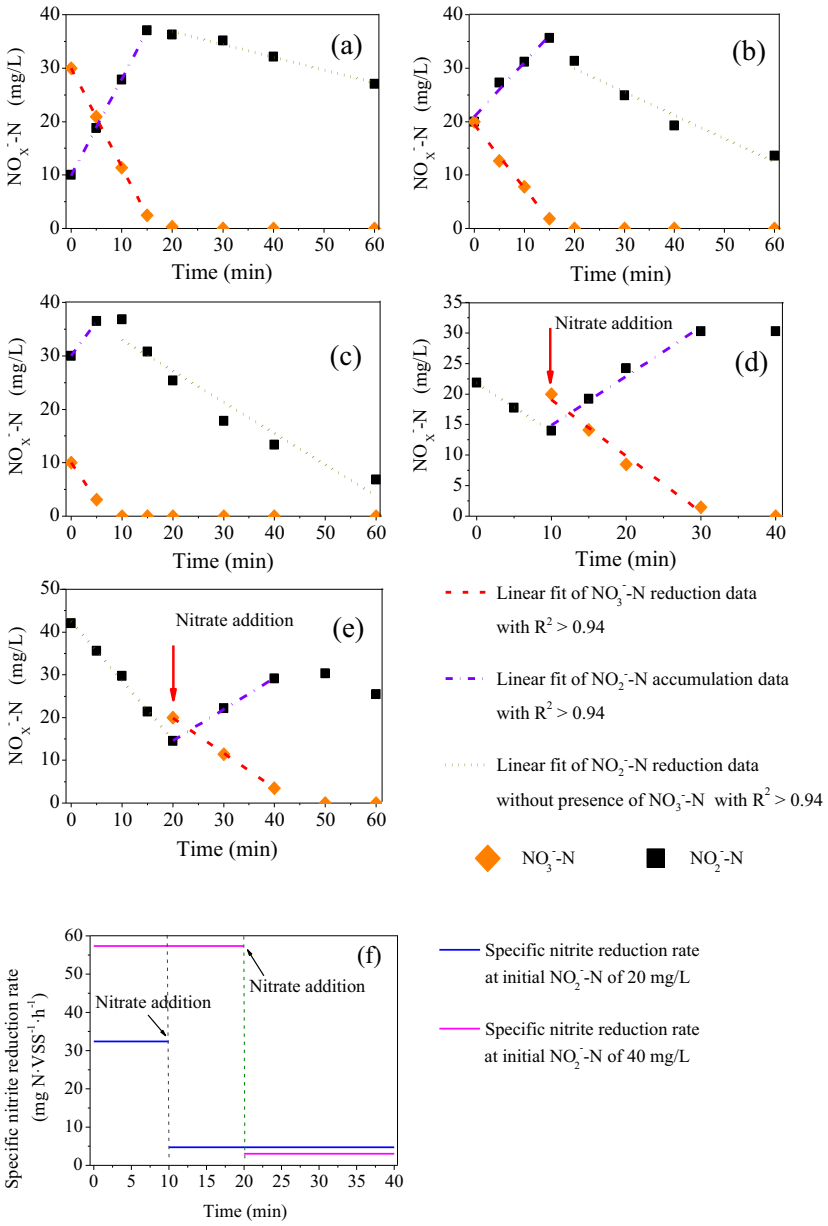

Fig. 5 Variation of NO_2^--N with NO_3^--N addition at different modes: **a** NO_3^--N/NO_2^--N=3:1, **b** NO_3^--N/NO_2^--N=1:1, **c** NO_3^--N/NO_2^--N=1:3, **d** initial NO_2^--N=20 mg/L, **e** initial NO_2^--N=40 mg/L, and **f** profiles of specific NO_2^--N reduction rate with NO_3^--N addition

inhibition of NO_2^--N reduction during denitrification process. Usually, NO_2^--N accumulation occurred under carbon-limiting conditions (Her and Huang 1995), which was possibly caused by the lower competitive capability of NO_2^--N reductase than NO_3^--N reductase for electrons, and the lower NO_2^--N reduction rate than NO_3^--N reduction rate. However, previous studies had found that higher C/N ratios could improve the NO_2^--N accumulation due to the temporary repression of NO_2^--N reductase from overcompetition with NO_3^--N reductase (Ge et al. 2012), which suggested that the

Table 2 Properties of partial denitrification with NO_3^--N addition

Tests	$\mu_{NO3\text{-}N}$ (mg N L^{-1} h^{-1})	$\mu_{NO2\text{-}N,\ Accu}$ (mg N L^{-1} h^{-1})	$\mu_{NO2\text{-}N}$ (mg N L^{-1} h^{-1})	$\acute{u}_{NO2\text{-}N}$ (mg N L^{-1} h^{-1})	$\acute{u}_{NO2\text{-}N}$ /$\mu_{NO2\text{-}N}$	NTR_B (%)
a	71.23	68.15	3.08	9.27	3.01	95.68
b	52.69	48.64	4.06	19.41	4.78	92.29
c	50.40	47.27	3.13	21.25	6.79	93.80
d	38.04	33.31	4.73	32.40	6.86	87.58
e	33.31	30.29	3.02	57.37	18.97	90.92

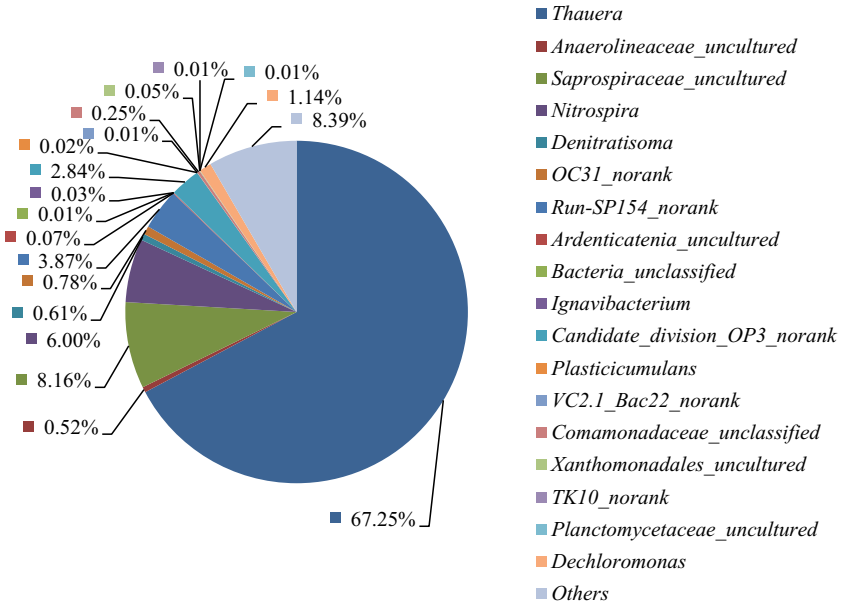

Fig. 6 Compositions of bacterial community in the partial denitrification SBR with high NO_2^--N accumulation classed by genus

competition for electrons between NO_2^--N reductase and NO_3^--N reductase would also take place with sufficient organic matters. In fact, NO_2^--N was regarded as the intermediate of NO_3^--N reduction and could accumulate. Previous studies of N_2O production with methanol utilizing denitrifying culture found that electron competition occurred no matter carbon sources were limited or abundant (Pan et al. 2013), indicating that the C/N ratio did not cause high NO_2^--N accumulation, and other factors should be considered, such as the operation condition and the shift of microbial community.

On the other hand, NO_2^--N accumulation was related to the type of carbon source. Previous study found that NO_2^--N was accumulated with acetate or propionate as the electron donor but was not accumulated in the presence of butyrate, valerate, or caproate (Rijn et al. 1996). This was explained by the difference in metabolism and electron flow velocity among the carbon sources, which caused different competitive power between NO_3^--N reductase and NO_2^--N reductase with different carbon source. Even wheb using the same carbon source, the competition for electron donor between NO_3^--N reductase and NO_2^--N reductase was different among denitrifying bacteria. Glucose resulted in the greatest NO_2^--N accumulation rate and production rate (Ge et al. 2012), while NO_2^--N accumulation did not occur when glucose was used with the sludge taking from SBR treating pre-treated landfill leachate (Sun et al. 2009). In this study, the high NO_2^--N accumulation was achieved using the sludge fermentation liquid as carbon source (Cao et al. 2013a), which contained a variety of short-chain fatty acids (e.g., acetic acid, propionic acid, and n-butyric acid), polysaccharide, and protein. The sludge fermentation liquid was later replaced by acetate; consequently, the property of high NO_2^--N accumulation did not degenerate, which indicated that the types of carbon source alone did not cause the discrepancy between NO_3^--N reductase and NO_2^--N reduction.

Previous studies found the conflicting roles of pH in NO_2^--N accumulation. The peak value of NO_2^--N accumulation increased when the pH increased from 7.5 to 9.0 in denitrification (Glass and Silverstein 1998). However, high peak values of NO_2^--N accumulation also occurred at a broader pH range (6.5~9.2) (Cao et al. 2013a). Moreover, the competition for electrons plays an important role on different nitrogen oxide reductases at low pH (6.0~6.5) (Pan et al. 2012). Therefore, the influence of pH on the nitrogen oxides was inconclusive and might not necessarily cause the competition between NO_3^--N reductase and NO_2^--N reductase. In this study, the pH was not controlled and varied from 7.5 to 8.5 in a typical cycle (Fig. 1b); correspondingly, the NTR_T showed little fluctuation during the NO_3^--N reduction period. This indicated that pH might not be a critical factor for high NO_2^--N accumulation in this study.

Furthermore, denitrification with NO_2^--N as the sole electron acceptor showed that NO_2^--N concentration declined linearly with time (Fig. 5d, e), which clearly indicated that the denitrifying bacteria were capable of reducing nitrite catalyzed by nitrite reductase enzymes. However, the NO_2^--N reduction rate sharply decreased when the NO_3^--N was present in the reactor (Fig. 5f), which suggested that the denitrifying bacteria preferred using NO_3^--N as the electron acceptor rather than NO_2^--N. It had been speculated that NO_2^--N accumulation was caused by three mechanisms: (1) imbalanced activities of NO_3^--N and NO_2^--N reductases, which are caused by C/N ratio, carbon source type, and pH; (2) inhibition of NO_2^--N reductase by oxygen, NO_3^-—N, or NO_2^-—N; and (3) selection and enrichment in favor of NO_3^--N respiring bacteria (Martienssen and Schöps 1997). The microbial community

enriched for facultative anaerobes for NO_3^--N reduction to NO_2^--N-sacrificed denitrifiers with glucose as organic carbon (Wilderer et al. 1987). It was speculated in this study that the anaerobic phase was related to bacterial enrichment with the intermediate NO_2^--N accumulation. In this case, the NO_2^--N reductase enzyme of these microorganisms was inhibited in the presence of NO_3^--N, which resulted in the difference between NO_3^--N reduction rate and NO_2^--N reduction rate.

Microbial community in high nitrite accumulation denitrifying sludge

NO_2^--N accumulation was strongly affected by the microbial species composition. There were some strains of bacteria known as incomplete denitrifying bacteria (nitrate-respiring bacteria), such as *Acidovorax facilis*, *Citrobacter diversus*, and *Enterobacter agglomerans*, which were only capable of reducing NO_3^--N to NO_2^--N without further reduction of NO_2^--N to N_2 and caused NO_2^--N accumulation (Glass and Silverstein 1998). These incomplete denitrifying bacteria lacked the key NO_2^--N reductase enzymes.

As to the denitrification system in this study, the most abundant genus was identified as *Thauera* (67.25 %) which was a member of *β-Proteobacteria* (Fig. 6). Most of the species within *Thauera* have been identified as denitrifiers (Srinandan et al. 2011). There were some strains of *Thauera* capable of reducing NO_3^--N to NO_2^--N under anaerobic condition (Liu et al. 2013a), which was consistent with the results in this study. Denitrification was subdivided into five functional groups (Drysdale et al. 2001), including true denitrifiers (bacteria capable of both NO_3^--N and NO_2^--N reduction), incomplete denitrifiers (bacteria that reduced NO_3^--N to NO_2^--N with no further reduction of NO_2^--N), incomplete nitrite reducers (bacteria capable of reducing both NO_3^--N and NO_2^--N but severe inhibition of NO_2^--N reduction by NO_3^--N), exclusive nitrite reducers (bacteria only capable of reducing NO_2^--N), and non-denitrifiers (bacteria incapable of reducing either NO_3^--N or NO_2^--N). It was assumed that the absolutely dominant *Thauera* genus in the partial denitrification with high NO_2^--N accumulation was possibly related to the NO_2^--N reduction inhibition in the presence of NO_3^--N, which was most likely caused by the asynchronism of denitrifying enzyme synthetization for different electron acceptors (NO_3^--N and NO_2^--N). Previous study demonstrated that the *nirS* mRNA in *Thauera* strains was not synthesized until NO_3^--N was consumed completely (Liu et al. 2013b). This was consistent with the result in the present study, which suggested that the high NO_2^--N in the partial denitrification system might be related to the dominant *Thauera* genus in microbial structure. NO_2^--N could be accumulated continuously and efficiently, since the NO_3^--N reductase was much more competitive for electron than NO_2^--N reductase.

Furthermore, *Saprospiraceae* groups were associated with the elimination of proteins (Xia et al. 2007). Bacteria belonging to *candidate division OP3* thrived in anoxic environment and were particle-associated (Glöckner et al. 2010; Liu et al. 2013b). *Comamonadaceae* (0.25 %) bacterium was identified in the systems assigned to PHA-degrading denitrifying bacteria (Khan et al. 2002) and produced slime extracellular polymeric substances (EPS) and capsular EPS (Bala Subramanian et al. 2010). *Dechloromonas* was reported to use benzene for reducing NO_3^--N to N_2 (Coates et al. 2001). These genera of bacteria identified in this study would be related to the endogenesis denitrification caused by the long idle phase (10.2~10.5 h) in a cycle, which implied that these bacteria might play an imported role in the aggregated growth, and contributed to the survival of biomass under substrate deficient condition and the long anaerobic period.

Additionally, there was relatively high amount of *Nitrospira* genus (6 %) in microbial community. Previous study had reported that the *Nitrobacter–Nitrospira* and *Nitrospira-nir*K showed a protocooperation relationship because they could eliminate the toxic effects of NO_2^--N when NO_2^--N accumulated and became excessive (Shu et al. 2015). In this study, NO_2^--N was accumulated at high NTR (90 %) with the presence of NO_3^--N, and the $\mu_{NO2\text{-}N,\ Accu}$ achieved 52.31 mg N VSS^{-1} h^{-1} even at the initial NO_3^--N of 20 mg/L (Table 1). The high amount of NO_2^--N accumulated could be used by both nitrite-oxidizing bacteria (NOB) (*Nitrospira*) and denitrifying bacteria. Thus, the presence of NOB could alleviate the negative effects of NO_2^--N accumulation on microorganisms.

Acknowledgments This study was supported by Natural Science Foundation of China (51478013) and The Thirteenth Science & Technology Program for the Graduate Students of BJUT (ykj-2014-11536).

Compliance with ethical standard

Ethical statement All of the authors declare that they have no conflict of interest. This article does not contain any studies with human participants or animals performed by any of the authors.

Reference

Almeida JS, Reis MAM, Carrondo MJT (1995) Competition between nitrate and nitrite reduction in denitrification by *Pseudomonas fluorescens*. Biotechnol Bioeng 46:476–484

APHA (1998) Standard Methods for the Examination of Water and Wastewater, 20th edn. American Public Health Association, Washington DC, USA

Bala Subramanian S, Yan S, Tyagi RD, Surampalli RY (2010) Extracellular polymeric substances (EPS) producing bacterial strains of municipal wastewater sludge: isolation, molecular dentification,

EPS characterization and performance for sludge settling and dewatering. Water Res 44:2253–2266

Blaszczyk M (1993) Effect of medium composition on the denitrification of nitrate by *Paracoccus denitrificans*. Appl Environ Microbiol 59: 3951–3953

Cao X, Qian D, Meng X (2013a) Effects of pH on nitrite accumulation during wastewater denitrification. Environ Technol 34:45–51

Cao S, Wang S, Peng Y, Wu C, Du R, Gong L, Ma B (2013b) Achieving partial denitrification with sludge fermentation liquid as carbon source: the effect of seeding sludge. Bioresour Technol 149:570–574

Coates JD, Chakraborty R, Lack JG, Ó Connor SM, Cole KA, Bender KS, Achenbach LA (2001) Anaerobic benzene oxidation coupled to nitrate reduction in pure culture by two strains of *Dechloromonas*. Nature 411:1039–1043

Drysdale GD, Kasan HC, Bux F (2001) Assessment of denitrification by the ordinary heterotrophic organisms in an NDBEPR activated sludge system. Water Sci Technol 43:147–154

Du R, Peng Y, Cao S, Wu C, Weng D, Wang S, He J (2014) Advanced nitrogen removal with simultaneous Anammox and denitrification in sequencing batch reactor. Bioresour Technol 162:316–322

Ge S, Peng Y, Wang S, Lu C, Cao X, Zhu Y (2012) Nitrite accumulation under constant temperature in anoxic denitrification process: the effects of carbon sources and COD/NO_3^--N. Bioresour Technol 114:137–143

Glass C, Silverstein J (1998) Denitrification kinetics of high nitrate concentration water: pH effect on inhibition and nitrite accumulation. Water Res 32:831–839

Glöckner J, Kube M, Shrestha PM, Weber M, Glöckner FO, Reinhardt R, Liesack W (2010) Phylogenetic diversity and metagenomics of *candidate division OP3*. Environ Microbiol 12:1218–1229

Gong L, Huo M, Yang Q, Li J, Ma B, Zhu R, Wang S, Peng Y (2013) Performance of heterotrophic partial denitrification under feast-famine condition of electron donor: a case study using acetate as external carbon source. Bioresour Technol 133:263–269

Her JJ, Huang JS (1995) Influence of carbon source and C/N ratio on nitrate/nitrite denitrification and carbon breakthrough. Bioresour Technol 54:45–51

Kalyuzhnyi S, Gladchenko M, Mulder A, Versprille B (2006) DEAMOX—new biological nitrogen removal process based on anaerobic ammonia oxidation coupled to sulphide-driven conversion of nitrate into nitrite. Water Res 40:3637–3645

Khan ST, Horiba Y, Yamamoto M, Hiraishi A (2002) Members of the family Comamonadaceae as primary poly (3-hydroxybutyrate-co-3-hydroxyvalerate)-degrading denitrifiers in activated sludge as revealed by a polyphasic approach. Appl Environ Microbiol 68: 3206–3214

Liu BB, Mao YJ, Bergaust L, Bakken LR, Frostegard A (2013a) Strains in the genus *Thauera* exhibit remarkably different denitrification regulatory phenotypes. Environ Microbiol 15:2816–2828

Liu G, Ling FQ, Magic-KnezevA LWT, Verberk JQJC, Van Dijk JC (2013b) Quantification and identification of particle-associated bacteria in unchlorinated drinking water from three treatment plants by cultivation-independent methods. Water Res 47:3523–3533

Ma B, Wang S, Zhu G, Ge S, Wang J, Ren N, Peng Y (2013) Denitrification and phosphorus uptake by DPAOs using nitrite as an electron acceptor by step-feed strategies. Front Env Sci Eng 7: 267–272

Martienssen M, Schöps R (1997) Biological treatment of leachate from solid waste landfill sites-Alterations in the bacterial community during the denitrification process. Water Res 31:1164–1170

Mulder A, van de Graaf AA, Robertson LA, Kuenen JG (1995) Anaerobic ammonium oxidation discovered in a denitrifying fluidized bed reactor. FEMS Microbiol Ecol 16:177–183

Ni BJ, Yu HQ (2008) An approach for modeling two-step denitrification in activated sludge systems. Chem Eng Sci 63:1449–1459

Oh J, Silverstein J (1999) Acetate limitation and nitrite accumulation during denitrification. J Environ Eng 125:234–242

Pan Y, Ye L, Ni BJ, Yuan ZG (2012) Effect of pH on N_2O reduction and accumulation during denitrification by methanol utilizing denitrifiers. Water Res 46:4832–4840

Pan Y, Ni BJ, Bond PL, Ye L, Yuan ZG (2013) Electron competition among nitrogen oxides reduction during methanol-utilizing denitrification in wastewater treatment. Water Res 47:3273–3281

Rijn JV, Tal Y, Barak Y (1996) Influence of volatile fatty acids on nitrite accumulation by a *Pseudomonas stutzeri* Strain isolated from a denitrifying fluidized bed reactor. Appl Environ Microbiol 62: 2615–2620

Shendure J, Ji HL (2008) Next-generation DNA sequencing. Nat Biotechnol 26:1135–1145

Shu D, He Y, Yue H, Wang Q (2015) Microbial structures and community functions of anaerobic sludge in six full-scale wastewater treatment plants as revealed by 454 high-throughput pyrosequencing. Bioresour Technol 186:163–172

Srinandan CS, Shah M, Patel B, Nerurkar AS (2011) Assessment of denitrifying bacterial composition in activated sludge. Bioresour Technol 102:9481–9489

Sun HW, Yang Q, Peng YZ, Shi XN, Wang SY, Zhang SJ (2009) Nitrite accumulation during the denitrification process in SBR for the treatment of pre-treated landfill leachate. Chinese J Chem Eng 17:1027–1031

Waki M, TomokoY FY, Kuroda K, Suzuki K (2013) Effect of electron donors on anammox coupling with nitrate reduction for removing nitrogen from nitrate and ammonium. Bioresour Technol 130:592–598

Wilderer PA, Jones WL, Dau U (1987) Competition in denitrification systems affecting reduction rate and accumulation of nitrite. Water Res 21:239–245

Xia Y, Kong Y, Nielsen PH (2007) In situ detection of protein-hydrolysing microorganisms inactivated sludge. FEMS Microbiol Ecol 60:156–165

Zhou Y, Oehmen A, Lim M, Vadivelu V, Ng WJ (2011) The role of nitrite and free nitrous acid (FNA) in wastewater treatment plants. Water Res 45:4672–4682

Zumft WG (1997) Cell biology and molecular basis of denitrification. Microbiol Mol Biol R 61:533–616